Applied Radiation and Isotopes 227 (2026) 112272

Contents lists available at ScienceDirect

Applied Radiation and Isotopes

journal homepage: www.elsevier.com/locate/apradiso

First intercomparison of ^{241}Am activity measurements using primary methods including magnetic micro-calorimetrers

Matias Rodrigues [a,*], Quentin Drenne [a], Frederic Juget [b], Miguel Roteta [c], Ole J. Nähle [d], Michael Müller [e], Sylvie Pierre [a], Lucille Chambon [a], Valérie Lourenço [a], Alexander Göggelmann [d], Marcell P. Takács [d], Martin Loidl [a], Karsten Kossert [d], Sebastian Kempf [e], Jörn Beyer [d], Marco Lombana [c], Virginia Peyrés [c], Ana Isabel Sánchez-Cabezudo [c]

[a] Université Paris-Saclay, CEA, LIST, Laboratoire National Henri Becquerel (LNE-LNHB), Palaiseau, F-91120, France
[b] Institut de Radiophysique, Lausanne, Switzerland
[c] Centro de Investigaciones Energéticas, Medioambientales y Tecnológicas, Madrid, Spain
[d] Physikalisch-Technische Bundesanstalt (PTB), Bundesallee 100, 38116, Braunschweig, Germany
[e] Institute of Micro- and Nanoelectronic Systems (IMS), Karlsruhe Institute of Technology (KIT), Hertzstrasse 16, 76187, Karlsruhe, Germany

ARTICLE INFO

Keywords:
Intercomparison
Magnetic micro-calorimeter
Activity standardization
Americium-241

ABSTRACT

Low-temperature detectors, such as Magnetic Micro-calorimeters (MMCs), exhibit several characteristics that make them strong candidates for primary activity standardization of various radionuclides. As a relatively new technique, however, many aspects of MMC-based measurements still require validation. For this purpose, ^{241}Am was selected to conduct an intercomparison of activity measurements between MMCs and other well-established conventional methods. The alpha-particle emitter ^{241}Am is well-suited to such comparisons, as it can be standardized with low uncertainty using a variety of techniques, including defined solid angle counting, coincidence counting, ionization chambers, and liquid scintillation counting (LSC). A key challenge in this context is the preparation of sources compatible with both MMCs and traditional standardization methods.

An ^{241}Am source was prepared by electro-precipitation in a specially designed geometry compatible with both multi-channel MMC spectrometry and conventional methods. This source was measured by four metrology institutes - LNE-LNHB, CIEMAT, CHUV, and PTB - using different primary methods. Subsequently, the original source was divided into 21 secondary sources, which were integrated into 11 absorbers of a multi-channel MMC spectrometer for the final activity determination.

Activity measurements using MMCs will be presented, along with the results of the intercomparison between different laboratories and techniques. The reported uncertainties are relatively high, in the range of a few percent, due to the rather low activity of the source and a potential loss of activity during the exercise. However, this first intercomparison provides insights and opportunities for improvement, which will be implemented in the future.

1. Introduction

Low-temperature detectors such as Magnetic Micro-calorimeters (MMCs) have many qualities that make them candidates as almost ideal detectors for primary activity standardization of a variety of radionuclides. With carefully designed setups, they combine up to 100 % detection efficiency, high energy resolution, and very low energy threshold. They can be suitable especially for low-energy pure beta-particle emitters as well as for electron-capture radionuclides, for which, until now, the activity standardization based on primarily methods such as liquid scintillation counting (LSC) (Broda et al., 2007) such methods require knowledge of certain nuclear and atomic decay data as input. As part of the *PrimA-LTD* project, a new method based on cryogenic detectors was developed with the objective of activity

This article is part of a special issue entitled: ICRM 2025 published in Applied Radiation and Isotopes.

* Corresponding author.
E-mail address: matias.rodrigues@cea.fr (M. Rodrigues).

https://doi.org/10.1016/j.apradiso.2025.112272
Received 30 June 2025; Received in revised form 3 October 2025; Accepted 13 October 2025
Available online 23 October 2025

determination with uncertainties of about 0.1 % for different decay modes (alpha decay, beta decay, and electron capture) (Müller et al., 2024).

A cryogenic detector consists of an absorber in which particles interact and deposit part or all of their energy, E. This results in a temperature increase, $\Delta T = E/C$, where C is the heat capacity of the detector. The quantity ΔT is converted into another physical quantity by a thermometer that is strongly thermally coupled to the absorber. The entire assembly is weakly coupled to a thermal bath so that the detector can return to its equilibrium temperature efficiently. Various sensor technologies exist depending on how the temperature change is transduced, among them the MMCs (magnetic micro-calorimeters) (Fleischmann et al., 2005). In this case, the thermometer is a paramagnetic sensor that converts the temperature change into a variation in magnetization. This change in magnetization is read with extremely high precision by a SQUID current sensor and through a superconducting flux transformer. Gold absorbers are well-suited for the use of MMCs — a high-Z metal that has the advantages of strong absorption of ionizing radiation, excellent thermalization and thermal conductivity, and chemical inertness, which is beneficial for source preparation. However, due to the high specific heat of gold, the operating temperature must be below 30 mK to minimize the absorber heat capacity C, which is crucial for high energy resolution. Since low temperatures also reduce noise, a good signal-to-noise ratio can be achieved for thermal cryogenic detectors.

Activity measurements with MMCs are carried out by decay energy spectrometry (DES) (Koehler, 2021). The source to be measured is enclosed within the gold absorber, which is dimensioned to achieve detection or counting efficiency as close as possible to 100 % for charged particles. Three major challenges arise in activity measurement using MMCs:

1. The volume of the absorber is constrained by a compromise between energy resolution and the absorber volume, i.e. its heat capacity. Typically, it should not exceed about a mm^3, which does not allow for the measurement of common traceable solid sources. These sources are generally prepared from a few tens milligrams of radioactive solutions in order to obtain a low mass uncertainty; this corresponds to a drop of a few tens mm^2.
2. Furthermore, it is currently not possible to deposit the especially small solution volumes (<10 μL) or the solution masses (<10 mg) required in such a way as to ensure traceability in Bq/g at a 0.1 % uncertainty level.
3. The rather large pulse decay time constants, in the order of a few milliseconds, limit the counting rate to only a few Bq per absorber since dead time and pile-up effects become more significant at higher activities.

To overcome two of these challenges (1 and 3), a reusable multichannel MMC module has been developed. The module is capable of measuring 10 MMC chips and 20 absorbers simultaneously. This allows a large surface area (~1 cm^2) primary source to be divided into multiple secondary sources (~a few mm^2 each) embedded in many absorbers and the primary source activity to be distributed among the absorbers.

The first step of the development of this system aims to validate activity measurement using the multichannel MMC module. To this end, a first intercomparison based on the measurement of the same ^{241}Am solid source by different methods and laboratories was carried out. Americium-241 offers several advantages: its alpha particles have high energies close to 5 MeV, but they are easily stopped and detected even in small absorbers. This eliminates concerns regarding detection threshold and detection efficiency of the MMCs. Furthermore, the activity of an ^{241}Am solid source can be measured using various methods (defined solid angle alpha counting (DSA), proportional counter, coincidence counting). The measurand for this intercomparison is the activity in becquerels (Bq). Once this step will have been validated, we can then focus on developing a new source deposition method for distributed and quantitative deposition in the absorbers, with traceability of the deposited mass, in order to perform mass activity measurements in Bq/g (Bergeron et al., 2023; Fitzgerald, 2025).

1.1. The ^{241}Am source

To carry out an intercomparison of activity measurements of the same source by both conventional techniques and MMCs, a pixelated ^{241}Am source was produced (Fig. 1). This allows the primary source to be easily divided into secondary sources, defined by pixels, with (in principle) minimal loss of activity. The primary source was first measured in its entirety using various conventional primary methods in the form as shown in Fig. 1. Then, it was cut around the pixels and the individual pixels were integrated into the absorbers of the multichannel MMC module. The fabrication details are presented in (Drenne, 2025).

The ^{241}Am source was electro-precipitated onto a 20 μm thick gold foil. That had been previously covered with a copper mask to guide local deposition of activity onto twenty-one pixels, each with a surface area of approximately 1 mm^2. The total activity of the source was only about 17 Bq because almost all the activity in the solution was deposited on the copper mask (800 Bq).

Another pixelated source was prepared during this work using a Kapton adhesive tape mask (not shown), but this source was not used due to poor deposition quality and mechanical instability, which posed a risk of activity loss and contamination (Drenne, 2025).

1.2. Activity measurements by well-established methods

The main objective of the intercomparison was to evaluate the activity of the same sample sent to the laboratories through primary or absolute procedures. Thus, this comparison exercise differs from the usual intercomparisons by sending the same source to each of the participants in a round robin format. Despite the precautions during transport and the use of appropriate packaging, significant changes can easily occur, especially a loss of activity, since there is no chemical bond to the substrate. The procedures involved in the intercomparison include:

1. Measurements in ionization chamber: ionization chambers are commonly used in radionuclide metrology for measuring radioactivity.
2. Defined solid angle measurements: this method involves measuring particles within a defined solid angle of the source-detector system, which is specially designed for this purpose. Assuming that all alpha particles which reach the detector are counted, the source activity can be obtained using the known solid angle.

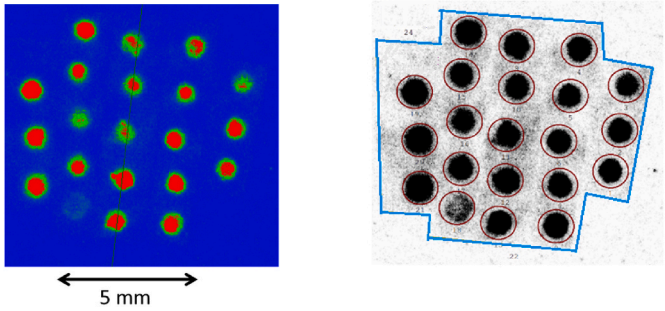

Fig. 1. Autoradiography images of the pixelated ^{241}Am source with different color maps and contrasts. On the right, the blue polygon represents the area of the primary source, and the dark red circles represent approximatively the area of the individual secondary sources to be obtained after subdivision. (For interpretation of the references to color in this figure legend, the reader is referred to the Web version of this article.)

3. Alpha-gamma coincidence counting: 4πα-γ coincidence counting refers to the detection of both alpha particles and gamma rays emitted from the same decay event. By determining the counting rates of detected alpha particles, gamma rays, and the alpha-gamma coincidences, one can determine the source activity without need for reference sources or nuclear decay data such as emission intensities.

The primary ^{241}Am source (pixelated as described in Section 1.1 and Fig. 1) was sent from the LNHB to the participating laboratories according to the following sequence: CIEMAT, CHUV, PTB to finally be returned to the LNHB.

The source remained at the CIEMAT for a month and a half and was measured using a 2π grid ionization chamber (IC), alpha-gamma coincidence counting (CC) in a pressurized proportional counter with a NaI (Tl) detector, and a defined solid angle (DSA) alpha particle counter.

The alpha-particle counting rate of the ^{241}Am source has been measured in a 2π grid ionization chamber (NUMELEC NU 14B). The area of each spectrum, including extrapolation to zero energy and background reduction, divided by the counting time is the counting rate of a measurement. The mean value of all the values is the counting rate, *Cr,* of the source. Since the solid angle of the geometry of measurement is 2π, the total counts, *Cr* must be multiplied by 2 and the activity *A* is calculated as $A = 2\,Cr/(1+B)$, where *B* is the backscattering contribution (Table 1). The backscattering coefficient was calculated using a software program called Crawford. This program calculates backscattering using input data consisting of the three main alpha-particle energies and the atomic weights of the support. The result was a backscattering coefficient of 1.42 % ($B = 0.0142$).

The sample was also measured within an 2πα-γ coincidence system. The experimental set-up consisted of a proportional counter pressurized to a pressure of 2×10^5 Pa and a NaI(Tl) detector. The polarization voltage is located in the region of the alpha plateau, so, since the electrons are not detected, no extrapolation was required (Table 1).

A complete description of the DSA with variable solid angle used at CIEMAT, as well as the method used to calculate the geometric efficiency, can be found in reference (García-Toraño et al., 2008). The detector distance was varied among 7.735 (2) cm, 8.734 (2) cm, and 9.734 (2) cm, corresponding to efficiencies of 2.52 (1) %, 2.001 (9) %, and 1.622 (7) %, respectively. The main source of uncertainty arises from the geometric factor, calculated as the quadratic sum of the uncertainties of each measurement. Additionally, there is a contribution from statistical counting, which is influenced by low efficiency, the low activity of the radioactive source, and a significant background in the detector. This uncertainty is calculated by considering the total count from the three measurements. Finally, the standard deviation of the three measured values is included (Table 1).

At the CHUV, the DSA method was used to measure the ^{241}Am source. The measurement vacuum chamber is an Alpha Analyst equipped with a PIPS detector of 450 mm^2 active surface (A 450-18-AM), both provided by Mirion. The chamber has a shelf that allows putting a sample holder at different distances from the detector. The sample is placed precisely at the center of the holder using a dedicated piece. The sample-detector distance is precisely measured using a dedicated tool and 4 different distances are used for the measurement: 1.848 (10) cm, 2.648 (10) cm, 3.448 (10) cm and 4.248 (10) cm. The geometrical efficiency for each distance was calculated using the autoradiography data provided by the LNHB using Legendre polynomials (Jaffey et al., 1954); the values obtained, are respectively, 7.85 %, 4.37 %, 2.75 % and 1.8 %. The final value of the activity is given by the arithmetic mean of the 4 measurements (Table 2). The uncertainty is given by the average quadratic sum of the uncertainty of each measurement plus the standard deviation of the four measured values (Table 2). Finally, the activity value obtained is 16.39 (0.13) Bq.

The PTB measured the source in a coincidence setup routinely used for 4πβ-γ-coincidence counting that was successfully employed for 2πα-γ-coincidence counting in the past. The system comprises a proportional counter operated at ambient pressure complemented by two NaI detectors, mounted above and below. Since both detectors differ significantly in the solid angle covered, any systematic effects might be revealed. The system uses digitizers for data acquisition and stores list-mode data for offline analysis using the PTB developed SoftKAM software package. The final result 16.9 (7) Bq was derived from about 16 days of continuous data taking in order to minimize the statistical uncertainty, which nevertheless is the dominating component (Table 3). It is mainly determined by statistics in the γ-channel and amounts to 0.61 Bq. A systematic difference in the results observed between the two NaI detectors was taken into account by assigning an uncertainty of 0.2 Bq.

Once the source returned to the LNHB, it was measured by DSA counting. This measurement lasted 13 days to reduce the statistical uncertainty (Table 4). The DSA counter used at LNHB employs a 2000 mm^2 PIPS detector (model PD, 2000–40 – 300 a.m. from Canberra/Mirion). The solid angle is defined by a slightly smaller collimator (diameter 40.510 (4) mm) and a relatively large source-collimator distance of 167.51 (10) mm. Dependent on the source geometry, its contribution to the activity uncertainty is typically of the order of 0.1 %. Due to the low source activity, combined with the small solid angle (geometry factor G = 0.3613 (13) %), the statistical uncertainty dominates in the DSA measurement. The relevant uncertainty components are summarized in Table 4. The value of the LNHB measurement by DSA is 16.57 (16) Bq at the reference date of April 15, 2023 12:00 U.T.C.

After all measurements, the primary source was divided into 21 secondary sources according to the distribution of activity among the pixels as described in Section 1.1. The activity was then measured by the LNHB's multi-channel MMC module.

1.3. Activity measurement using MMCs

The multichannel MMC module was developed as part of the *PrimA-LTD* project. It is composed of optimized MMC chips produced through microfabrication by KIT Karlsruhe (Müller et al., 2024) (Fig. 2). These chips contain the planar pickup coils of the flux transformer and the paramagnetic sensors. Two pickup coils are connected in parallel to the input coil of the SQUID, so that one SQUID chip measures two absorbers, which can be distinguished by the opposite polarities of the pulses (positive and negative). The sensors are thermally coupled with gold pads whose function is to thermally connect the absorber to the sensor

Table 1
Measurement results and uncertainty budgets (k = 1) obtained for the ^{241}Am source at CIEMAT by IC, and CC and DSA.

	IC	DSA	CC
Activity (Bq)	**16.92**	**16.28**	**17.0**
Uncertainty (Bq)	**0.09**	**0.15**	**0.6**
Statistics	0.4 %	0.20 %	3.0 %
Geometrical factor	–	0.83 %	–
Standard deviation of the three measured values	–	0.27 %	–
Background	0.3 %		1.8 %
Total	**0.5 %**	**0.90 %**	**3.53 %**

Table 2
Measurement results and uncertainty budgets (k = 1) obtained for the ^{241}Am source at the CHUV by DSA.

	Pos5	Pos7	Pos9	Pos11
Activity (Bq)	**16.37**	**16.31**	**16.43**	**16.47**
Uncertainty	**Pos5**	**Pos7**	**Pos9**	**Pos11**
Statistics	0.60 %	0.48 %	0.49 %	0.28 %
Geometrical factors	0.82 %	0.65 %	0.53 %	0.44 %
Detector diameter	0.65 %	0.73 %	0.77 %	0.79 %
Centering	0.55 %	0.36 %	0.24 %	0.17 %
Total	**1.33 %**	**1.15 %**	**1.08 %**	**0.97 %**

Table 3
Uncertainty budgets (k = 1) obtained for the ^{241}Am source at the PTB by 4πβ-γ-coincidence counting.

Component	Uncertainty in %
Statistics	3.6
Background	0.62
γ-Detector	1.2
γ-Threshold	0.25
Deadtime correction	0.1
Coincidence time	0.1
Total	**3.9**

Table 4
Results and uncertainty budget (k = 1) for the two DSA measurements at LNHB.

Activity (Bq)	**16.57**
Uncertainty (Bq)	**0.16**
Statistics	0.41 %
Tailing	0.14 %
Geometry factor	0.083 %
Backscattering on chamber wall	0.10 %
Total	**0.46** %

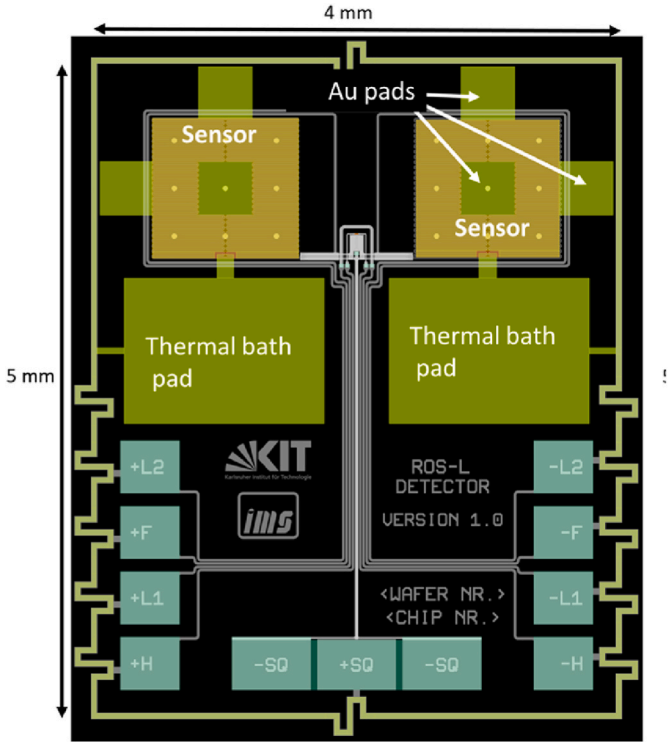

Fig. 2. Layout of the MMC chip RoS L. Two absorbers are thermally connected to the two sensors via the gold pads. The MMC chip is read out by a SQUID chip connected to the bond pads± SQ. (For interpretation of the references to color in this figure legend, the reader is referred to the Web version of this article.)

using gold bonding wires via ultrasonic welding. For the MMC chips *RoS-L*, three gold pads are connected to the sensor—one central pad and two lateral pads. The absorber can be easily detached from these pads to allow reuse of the MMC chips and the module for other absorber measurements.

Twelve absorbers were prepared; eleven of them contained the 21 secondary sources. Ten of these absorbers contain two sources each whose activities, extracted from the autoradiography, were combined in a way that minimizes the scatter of the total activities between the absorbers. The twelfth absorber, without any source, is used as a blank to monitor the background. The sources were enclosed between two 100 μm-thick gold foils. This thickness was chosen to achieve a detection efficiency of more than 99.9 % when integrating the number of events over a region of interest including $E1 = 5.570$ MeV and $E2 = 5.634$ MeV. The energy *E2* corresponds to the full energy peak, i.e., the *Q*-value of the ^{241}Am decay when all emitted particles are absorbed. The energy *E1* corresponds to the transition energy *Q* minus the gamma transition energy of about 60 keV, i.e. when corresponding gamma rays escape.

Two secondary source foils were placed between the two absorber sheets, with a surface area of 2.5 × 2.5 mm^2. The stack was sealed by diffusion bonding using a press at 400 °C for 2 h. The absorbers were coupled to the sensors using one of the side pads and about 10 gold wires of 25 μm diameter and a length of 0.5 mm (see inset in Fig. 3). The twelve absorbers are grouped into six pairs, each associated with one MMC chip and one SQUID chip (Fig. 3). The absorbers of a pair produce pulses with opposite polarities.

The multi-channel module was mounted in the dilution refrigerator of the LNHB and cooled to approximately 15 mK. At this temperature, the pulse time constants were found to be much longer than expected: about 500 μs for the rise time, and about 60 ms for the decay time. Although the activity per absorber is only 1–2 Bq, this significantly increased the dead time percentage from 30 % to 50 %. Therefore, a second measurement was performed at around 80 mK. This reduced the time constants to about 100 μs and 20 ms, and consequently the dead time decreased significantly to less than 20 %.

Two analysis methods were applied to determine the activity. The first one (counting method) is simply counting the number of events above the detection thresholds. The second one (spectrometric method) measures the activity as the number of events within a Region of Interest (ROI), between the energies *E1* and *E2*, including the two main peaks of the spectrum (Fig. 4). For both methods, two trigger thresholds (positive and negative) were set to identify pulses of opposite polarity from the two absorbers of a pair. Additionally, an extendable dead time was applied with the specific feature that the dead time window was proportional to the duration that the pulse remains above the threshold, and thus to its amplitude. Saturation events were also detected; in such cases, a fixed dead time window of 100 ms was applied.

The main difference between the two methods is in the treatment of pile-up in using the spectrometric methods. When a pulse is detected, a second pulse may pile-up on the detected pulse decay and the measured energy is altered and falls outside of the ROI. To correct for these out-of-ROI events, the live time is multiplied by the probability that no additional pulse occurs during the pulse decay and the associated energy processing window. This probability, about 1 %, is calculated using a Poisson distribution and the observed counting rate per absorber.

Table 5 compares the counting rates obtained with both methods. For all 11 absorbers, the counting rates are consistent within uncertainties. The measured activity is the sum of the counting rates from the 11 absorbers, minus 11 times the rate observed in the reference 12th absorber (blank), for which the correction is negligible. The Type A uncertainty includes the statistical counting uncertainty. An uncertainty related to the counting analysis was calculated. For the counting method, this uncertainty is due to the detection threshold. Although the pulses are well above threshold, pile-up between a positive pulse and a negative pulse may occur; if they are in coincidence, the measured energy is, therefore, close to zero and falls below the threshold. This uncertainty does not affect the spectrometric method, but instead, a counting analysis uncertainty related to the live time correction and the pile-up events out of the ROI was chosen.

The activity measured at 80 mK by the MMCs was 15.897 (11) Bq, with an excellent agreement between the two analysis methods. At 15 mK, the spectrometric method shows a slight disagreement; the large dead time and too low thresholds for some absorbers may have affected this analysis.

The initial activity obtained using the MMCs shows a significant discrepancy compared to the results from the conventional methods.

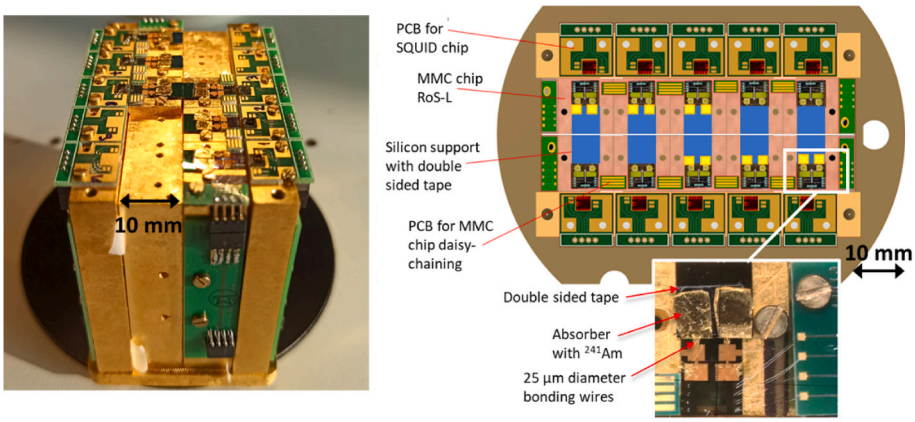

Fig. 3. Left, photograph of the multichannel MMC module with six MMC chips and six SQUID chips installed. Right, top view of the module layout with the maximum of ten chips each in place (electrical connections via bonding wires are not shown). The inset shows a close-up photograph of one of the channels with its two absorbers containing ^{241}Am.

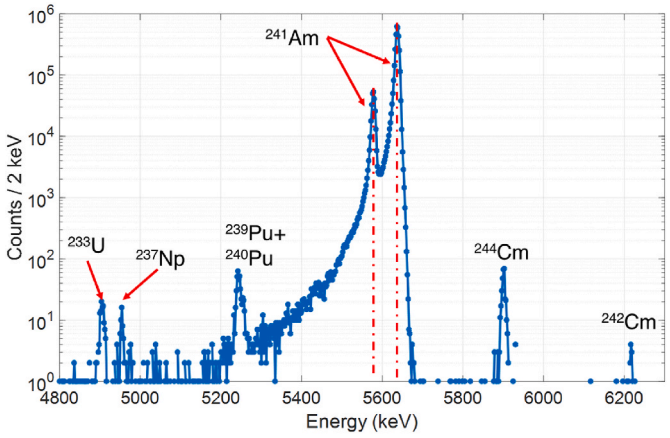

Fig. 4. Combined decay energy spectrum of the 11 absorbers measured at 15 mK. The vertical dashed lines mark the position of the energies *E1* and *E2*.

This bias originated from the preparation of the secondary sources. Initial autoradiographs were mistakenly interpreted as there was no activity between the pixels, which was later shown to be incorrect. Changing the contrast of the autoradiography revealed contamination between pixels (Fig. 1), which had been counted as part of the activity during the primary source measurement but was partially lost during the preparation of the secondary sources.

To confirm this hypothesis, the lost activity was estimated based on autoradiographic images. The maximum and minimum fractions of lost activity were determined by defining minimal and maximal cutting contours around the secondary sources (Fig. 1). The average lost activity was estimated at 6.5 (14) %. The Type B uncertainty associated with this source correction was evaluated assuming a rectangular distribution, bounded by the minimum and maximum estimated losses. This correction adds a major additional uncertainty to the MMC measurement (Table 5).

Of particular interest is the decay energy spectrum in Fig. 4, which demonstrates a remarkable ability to detect the presence of impurities like no other technique. The spectrum reveals the presence of ^{233}U, ^{239}Pu, ^{240}Pu, ^{237}Np, ^{242}Cm, and ^{244}Cm, as low as 4 ppm of ^{242}Cm relative to ^{241}Am. The total activity of the impurities, 4.5 mBq, was treated as a Type B uncertainty (Table 5).

1.4. Results

The key comparison reference value, based upon the calculation of the power-moderated mean (PMM) of the results obtained by the different techniques, is 16.67 (6) Bq. Table 6 summarizes the activity values obtained by each laboratory and each technique and Fig. 5 illustrates the comparison results. The MMC result is in agreement with other results after correction for activity loss, with stated uncertainties.

2. Conclusions and perspectives

Although this first intercomparison did not meet the targeted objectives, namely a comparison between different activity measurement

Table 6
Results and uncertainties (k = 1) obtained by the different laboratories and methods (CC, IC, DSA, and MMC after correction).

Laboratory (method)	Activity (Bq)	Uncertainty (Bq)
CIEMAT (CC)	17.0	0.6
CIEMAT (IC)	16.92	0.09
CIEMAT(DSA)	16.28	0.15
PTB (CC)	16.9	0.7
CHUV (DSA)	16.39	0.13
LNHB (DSA)	16.57	0.16
LNHB (MMC) corr.	16.87	0.22
PMM value	**16.67**	**0.06**

Table 5
Results and uncertainties (k = 1) of the activity measurement of the ^{241}Am source using MMCs. The activity uncertainty before the correction of the source preparation comprises all the uncertainty contributions excepted the one from the source correction.

Temperature	Analysis method	Activity before correction (Bq)	Activity after correction (Bq)	Unc. Type A (Bq)	Unc. Type B (Bq)		
					Counting analysis	Impurity	Source correction
15 mK	Counting	15.873 (14)	16.90 (22)	8.9×10^{-3}	8.9×10^{-3}	7.2×10^{-3}	2.2×10^{-1}
	Spectro.	15.845 (12)	16.87 (22)	8.9×10^{-3}	5.0×10^{-3}	7.2×10^{-3}	2.2×10^{-1}
80 mK	Counting	15.897 (11)	16.93 (22)	7.6×10^{-3}	3.8×10^{-3}	7.2×10^{-3}	2.2×10^{-1}
	Spectro.	15.896 (12)	16.86 (22)	7.6×10^{-3}	5.9×10^{-3}	7.2×10^{-3}	2.2×10^{-1}

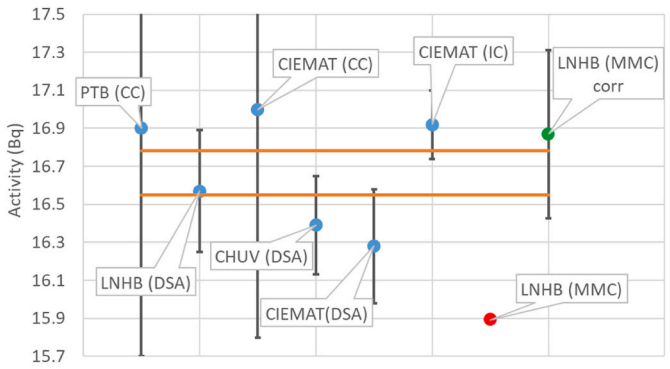

Fig. 5. Activity results obtained by the different laboratories and methods with a coverage factor k = 2 (CC: coincidence counting; IC: ionization chamber; DSA: defined solid angle counting; MMC: magnetic micro-calorimeter). The two values for MMC are without and with the correction of the activity loss during the source preparation. The orange lines give the limits around the PMM value with a coverage factor k = 2. (For interpretation of the references to color in this figure legend, the reader is referred to the Web version of this article.)

methods having uncertainties on the order of 0.1 %, it does give valuable insights.

For conventional methods, the uncertainties were dominated by the low activity of the primary source, nominally 17 Bq. However, such a low activity is well suited for analysis by MMC spectrometry, as the pulse time constants were abnormally long, leading to a large dead time fraction. The uncertainty of the present MMC measurement is dominated by a bias that had to be corrected *a posteriori* due to an incorrect initial assumption that there was no activity between the pixels of the secondary sources. The need for such a correction may be avoided only with an improved sample preparation methodology.

Despite this, the intercomparison validated several experimental aspects. An intercomparison protocol was successfully implemented for an activity measurement by transporting a source among different laboratories to compare different measurement methods. In addition, the multi-channel MMC module was successfully operated with six functional channels, which will later be extended to ten. The data processing and the analysis of the MMC measurement were validated using two different counting methods. This measurement also helped to identify experimental limitations that need to be addressed such as needs to improve sample preparation techniques. A second intercomparison is currently underway. For this new campaign, the primary source will have an activity of approximately 1 kBq to reduce the statistical uncertainties of the activity measurement by conventional methods. The challenge then becomes counting an activity of the order of 100 Bq per MMC absorber. The pulse time constants of the MMC will be reduced, firstly, by decreasing the absorber heat capacity so that only alpha particles are detected (ignoring photon escapes), which will correspond to a wider ROI of analysis; secondly, the causes of the excessively long pulse time constants, which have already been identified, will be solved. Under these conditions, simulations have shown that a counting rate of 100 s^{-1} is achievable with our MMCs. Finally, the preparation of the secondary sources cut-out from the primary source will be revised to avoid the need for a correction whose uncertainty currently dominates the MMC measurement.

CRediT authorship contribution statement

Matias Rodrigues: Writing – original draft, Validation, Methodology. **Quentin Drenne:** Investigation, Data curation, Conceptualization. **Frederic Juget:** Writing – original draft, Validation, Investigation. **Miguel Roteta:** Writing – original draft, Validation, Investigation. **Ole J. Nähle:** Writing – original draft, Validation, Project administration, Investigation, Funding acquisition. **Michael Müller:** Investigation, Conceptualization. **Sylvie Pierre:** Validation, Investigation. **Lucille Chambon:** Writing – review & editing, Investigation. **Valérie Lourenço:** Investigation. **Alexander Göggelmann:** Investigation. **Marcell P. Takács:** Investigation. **Martin Loidl:** Writing – review & editing. **Karsten Kossert:** Resources, Methodology. **Sebastian Kempf:** Project administration, Funding acquisition. **Jörn Beyer:** Conceptualization. **Marco Lombana:** Investigation. **Virginia Peyrés:** Validation, Investigation, Conceptualization. **Ana Isabel Sánchez-Cabezudo:** Validation, Investigation.

Declaration of competing interest

The authors declare that they have no known competing financial interests or personal relationships that could have appeared to influence the work reported in this paper.

Acknowledgements

This work has received funding from the EMPIR project 20FUN04 *PrimA-LTD*, co-financed by the Participating States and from the European Union's Horizon 2020 research and innovation program.

Data availability

Data will be made available on request.

References

Bergeron, D.E., Essex, R., Nour, S., Shaw, G.A., Verkouteren, R.M., Fitzgerald, R.P., 2023. Gravimetric deposition of microliter drops with radiometric confirmation. In: Applied Radiation and Isotopes, 201. Elsevier BV, 111025. https://doi.org/10.1016/j.apradiso.2023.111025.

Broda, R., Cassette, P., Kossert, K., 2007. Radionuclide metrology using liquid scintillation counting. Metrologia 44, S36–S52.

Drenne, Q., et al., 2025. Source preparation of ^{241}Am and ^{129}I for MMC absorbers of a multi-channel decay energy spectrometer. Appl. Radiat. Isot. 226, 112184. https://doi.org/10.1016/j.apradiso.2025.112184.

Fleischmann, A., Enss, C., Seidel, G. Metallic magnetic calorimeters. In: Enss, C. (eds) 2005 Cryogenic Particle Detection. Topics in Applied Physics, vol 99. Springer, Berlin, Heidelberg. https://doi.org/10.1007/10933596_4.

Fitzgerald, R.P., et al., 2025. Primary activity measurement of an Am-241 solution using microgram inkjet gravimetry and decay energy spectrometry. Metrologia 62, 045005. https://doi.org/10.1088/1681-7575/adecaa.

García-Toraño, E., et al., 2008. Defined solid-angle counter with variable geometry. Appl. Radiat. Isot. 66, 881–885. https://doi.org/10.1016/j.apradiso.2008.02.040.

Jaffey, A.H., 1954. Solid angle subtended by a circular aperture at point and spread sources: formulas and some tables. Rev. Sci. Instrum. 25 (4), 349–354.

Koehler, Katrina Elizabeth, 2021. Low Temperature Micro-calorimeters for Decay Energy Spectroscopy. Web, United States: N. https://doi.org/10.3390/app11094044 (0123456789).

Müller, M., Rodrigues, M., Beyer, J., et al., 2024. Magnetic micro-calorimeters for primary activity standardization within the EMPIR project PrimA-LTD. J. Low Temp. Phys. 214, 263–271. https://doi.org/10.1007/s10909-024-03048-7.